

Field emission properties of self-assembled silicon nanostructures on *n*- and *p*-type silicon

S. Johnson^{a)} and A. Markwitz^{b)}

Rafter Research Centre, Institute of Geological and Nuclear Sciences, P.O. Box 31-312,
30 Gracefield Road, Lower Hunt, New Zealand

M. Rudolphi and H. Baumann

Institute for Nuclear Physics, J. W. Goethe-University, August-Euler-Str. 6, 60486 Frankfurt, Germany

S. P. Oei, K. B. K. Teo, and W. I. Milne

Department of Engineering, University of Cambridge, Trumpington Street, Cambridge, CB2 1PZ,
United Kingdom

(Received 9 April 2004; accepted 18 August 2004)

This letter considers field emission from self-assembled silicon nanostructure arrays fabricated on *n*- and *p*-type silicon (100) substrates using electron beam rapid thermal annealing. Arrays of nanostructures with an average height of 8 nm were formed by substrate annealing at 1100 °C for 15 s. Following conditioning, the Si nanostructure field emission characteristics become stable and reproducible with Fowler–Nordheim tunneling occurring for fields as low as 2 V μm^{-1} . At higher fields, current saturation effects are observed for both *n*-type and *p*-type samples. These studies suggest that the mechanism influencing current saturation at high fields acts independently of substrate conduction type. © 2004 American Institute of Physics. [DOI: 10.1063/1.1804604]

In a previous study we demonstrated the growth of silicon nanowhiskers on untreated Si(100) using electron beam rapid thermal annealing (EB-RTA).^{1,2} Nanowhisker growth is initiated by decomposition of the native oxide layer which is well known to undergo thermal decomposition in environments of low oxygen partial pressure.^{3,4} Decomposition occurs through the formation of voids in the oxide film which enlarge laterally across the surface, coalesce, and finally extend over the entire substrate leaving the surface oxide free. Void growth occurs via the interfacial reaction $\text{Si} + \text{SiO}_2 \rightarrow 2\text{SiO}\uparrow$, where the silicon species are provided by mobile silicon monomers which diffuse to the void perimeter in order to react with the oxide layer. This mechanism results in consumption of silicon from the void regions and results in atomic scale surface disorder.

As annealing continues, diffusive Si species generated both thermally and by electron stimulated desorption processes⁵, migrate across the oxide free surface in response to the strained potential-energy surface resulting from the surface disorder. Oshiyama⁶ showed an increase in energy for adatom diffusion at the upper edge of a step. This potential barrier tends to promote bunching of steps once the flow of the step is pinned at a given site. A pit in a step terrace, as created in the disordered silicon surface following oxide decomposition, acts as such a pinning site resulting in the growth of islands around the pinning site. The size and number (surface density) of islands evolve as further adatoms are incorporated into the islands supplied either from the adatom sea between islands or from smaller islands which act as feed stock for the larger islands.⁷ The small apex radius of the resulting nanowhiskers and the ease of fabrication make

these ideal structures for the study of field emission phenomena from nano-scale cathodes.

The field emission characteristics of nanowhiskers formed on *n*-type (Sb-doped, 0.07–0.09 $\Omega\text{ cm}$) and *p*-type [B-doped, 1–10 $\Omega\text{ cm}$] silicon (100) substrates was performed in a parallel plate diode configuration. Electrical isolation and cathode–anode separation was achieved using a 100- μm -thick PTFE film, and measurements were performed under vacuum of 1×10^{-6} mbar. Samples were prepared by EB-RTA at 1100 °C for 15 s and with electron beam energy of 20 keV. The resulting nanowhiskers exhibit an average height of 8 nm and a surface density of 11 μm^{-2} , independent of conductivity type. Typical AFM images of the *n*- and *p*-type surface are shown in Figs. 1(a) and 1(b), respectively. It was found necessary to run several emission cycles in order for the *I*–*E* characteristics to become stable and repro-

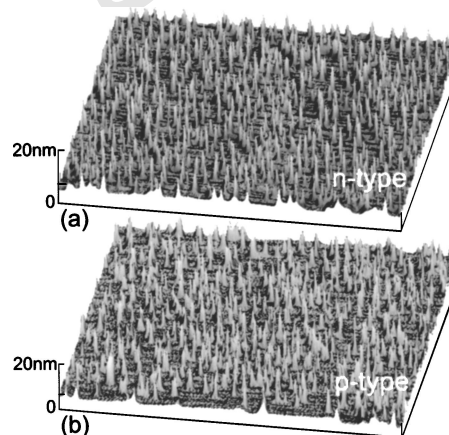


FIG. 1. 8 $\mu\text{m} \times 8 \mu\text{m}$ AFM surface plots for nanowhiskers formed on (a) *n*-type silicon (100) and (b) *p*-type silicon (100) substrates, respectively. In both cases the nanowhiskers were formed following electron beam rapid thermal annealing of the untreated substrate at 1100 °C (temperature gradients ± 5 °C/s) for 15 s.

^{a)}Author to whom correspondence should be addressed; electronic mail: s.johnson@gns.cri.nz

^{b)}Also at: The MacDiarmid Institute for Advanced Materials and Nanotechnology, Victoria University of Wellington, New Zealand.

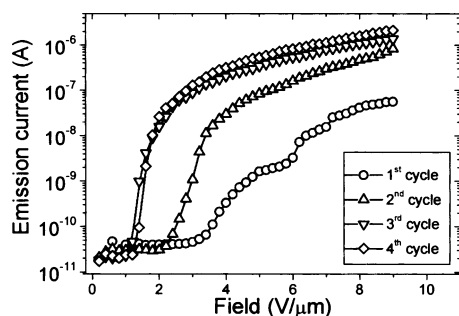


FIG. 2. Semi-logarithmic plot of I - E field emission characteristics for nanowhiskers formed on p -type substrate. The four curves correspond to successive anode voltage cycles, where cycle 1 corresponds to the first emission experiment and cycle 4 the final.

ducible. The I - E characteristics plotted in Fig. 2 show the change in emission current for four successive electron emission cycles for nanowhiskers formed on p -type Si substrates. The electric field is the average, macroscopic value calculated from the ratio of the applied voltage to cathode-anode separation and thus does not include local field enhancement due to surface geometry. The emitter array was maintained under vacuum between successive cycles. The total emission current for a given applied field increases significantly between the first and second cycles, with the increase in current becoming smaller with successive cycles. Further, the threshold field, which we define as the macroscopic field required to detect a current of 1 nA, was found to reduce from 4 to 2 $\text{V } \mu\text{m}^{-1}$ between the first and final cycle, respectively. These values are considerably lower than that observed for conventional microfabricated Si cathodes,⁸ which typically exhibit a threshold field value around 20 $\text{V } \mu\text{m}^{-1}$, and is believed to be a result of significant localized field enhancement at the apex of the nanowhiskers. The two curves describing the third and fourth cycles are approximately identical indicating a steady state. Improvements of emission characteristics over time are common for field emission phenomena from silicon cathodes.⁹

Current-field (I - E) characteristics of the n - and p -type nanostructured Si surfaces following an identical period of conditioning are shown in Fig. 3. Three distinct regions can be seen for both materials corresponding to the zero emission, field emission, and current saturation regions, respectively. Plotting the I - E characteristics of region 2 on a Fowler-Nordheim plot [$\ln(I/E^2)$ vs E^{-1}], as shown in the inset of Fig. 3, gives a straight line for both n - and p -type

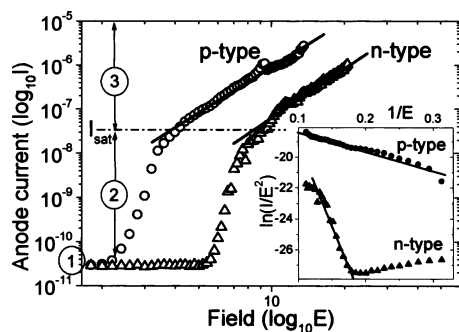


FIG. 3. Logarithmic plot of I - E field emission characteristics measured in a diode configuration for nanowhiskers formed on n - and p -type substrates. The corresponding Fowler-Nordheim plots [$\ln(I/E^2)$ vs E^{-1}] are shown in the inset.

emitters suggesting a Fowler-Nordheim tunneling process. A difference in the threshold field for electron emission from nanowhiskers formed on n - and p -type substrates was observed, with emission from p -type Si substrates consistently occurring at a lower macroscopic field. The substantial similarities between the average aspect ratio and spatial arrangement of nanowhiskers formed on n - and p -type substrates, suggests that localized field enhancement due to geometric differences cannot account for this observation. The difference in threshold field has been attributed to the formation of a potential barrier in the n -type cathodes due to the existence of negatively charged surface states.¹⁰ Because of the large effective surface area of the nanowhiskers we may expect a high density of such surface states. Band-bending acts oppositely in p -type Si, and thus there exists no surface potential barrier for electron transport to the emission site.

At high electric fields (region 3 of Fig. 3) electron emission from both substrates exhibit a saturation region in the I - E plot. Microfabricated p -type Si cathodes show current saturation phenomena related to the limited supply of electrons, the minority carriers, within the tip.¹¹ Supply limited emission is also observed for n -type cathodes,¹² however, due to the greater electron density in the conduction band, the onset of current saturation typically occurs at larger emission currents than that observed for geometrically identical p -type cathodes. This is inconsistent with the experimental result presented here which indicates the onset of current saturation occurs concurrently at an emission current, I_{sat} .

Current saturation may also be related to the accumulation of charge, either in the surface region and/or in the vacuum region between cathode and anode.¹³ Such space charge limited conduction mechanisms are typically revealed by a relationship of the form $I = kE^n$, where $n > 1$, which yields a straight line when the I - E characteristics are plotted on logarithmic axis.¹⁴ Both the n - and p -type substrates show evidence of such a relationship, as shown in region 3 of Fig. 3. The lines shown in Fig. 3 were found to be the best fit of the experimental data with correlation coefficients, $R^2 = 0.99$ for both cases. The relationships between I and E for the n - and p -type nanowhisker diode operating in the saturation region were $I \propto E^{3.3}$ and $I \propto E^{3.5}$, respectively. Models based on other current conduction mechanisms, specifically Fowler-Nordheim tunneling, Schottky emission, and Poole-Frenkel conduction mechanisms were also assessed. Space charge limited conduction was found to best describe conduction in the saturation region. It should be noted that although the current saturation mechanism is dominated by space charge limited conduction, other secondary mechanisms may also contribute to current saturation. The good agreement in the values of the exponent, n , for the n - and p -type substrates indicates that the space charge current limiting mechanism is largely independent of the substrate conduction type, and is likely related to commonalities in the nanowhisker structure or the experimental geometry.

In conclusion, the possibility of using self-assembled nanostructure arrays formed on n - and p -type silicon (100) substrates as field emission cathodes has been demonstrated. Following conditioning the field emission characteristics are stable and reproducible with emission occurring at very low threshold fields. At high fields the emission current deviates from Fowler-Nordheim tunneling and becomes limited by space charge, providing an intrinsic method for cathode protection.

The authors would like to express their thanks to Associate Professor R. Blaikie, and H. Devereux from the University of Canterbury for assistance with the AFM analysis. This work was performed under research contracts to the New Zealand Foundation for Research, Science and Technology (C05X0008, "Advanced industrial materials at the nanoscale").

¹S. Johnson, A. Markwitz, M. Rudolphi, and H. Baumann, *J. Appl. Phys.* (to be published).

²A. Markwitz, H. Baumann, E. F. Krimmel, and K. Bethge, *Appl. Phys. Lett.* **64**, 2652 (1994).

³R. Tomp, G. W. Rubloff, P. Balk, F. K. LeGoues, and E. J. van Loenen, *Phys. Rev. Lett.* **55**, 2332 (1985).

⁴K. Hofmann, G. W. Rubloff, and R. A. McCorkle, *Appl. Phys. Lett.* **49**, 1525 (1986).

⁵K. Nakayama and J. H. Weaver, *Phys. Rev. Lett.* **82**, 980 (1999).

⁶A. Oshiyama, *Phys. Rev. Lett.* **74**, 130 (1995).

⁷P. W. Voorhees, *Annu. Rev. Mater. Sci.* **22**, 197 (1992).

⁸T. Sugino, S. Kawasaki, K. Tanioka, and J. Shirafuji, *Appl. Phys. Lett.* **71**, 2704 (1997).

⁹A. J. Miller and R. Johnston, *J. Phys.: Condens. Matter* **3**, 231 (1991).

¹⁰T. Matsukawa, S. Kanemaru, K. Tokunaga, and J. Itoh, *J. Vac. Sci. Technol. B* **18**, 1111 (2000).

¹¹E. C. Boswell and P. R. Wilshaw, *J. Vac. Sci. Technol. B* **11**, 412 (1993).

¹²M. Ding, H. Kim, and A. I. Akinwande, *Appl. Phys. Lett.* **75**, 823 (1999).

¹³J. P. Barbour, W. W. Dolan, J. K. Trolan, E. E. Martin, and W. P. Dyke, *Phys. Rev.* **92**, 45 (1953).

¹⁴P. Gonon, A. Deneuve, F. Fontaine, and E. Gheeraert, *J. Appl. Phys.* **78**, 6633 (1995), and references therein.